Electronic Supplementary Information

In situ Loading Ag Nanocontacts onto Silica Nanospheres: A SERS Platform for

Ultrasensitive Detection

Yubian Han,[a,b] Shengjun Liu,[a,b] Bianhua Liu Changlong Jiang[b*] and Zhongping Zhang [a,b*]

[a] Department of Chemistry, University of Science & Technology of China, Hefei, Anhui, 230026, China.
[b] Institute of Intelligent Machines, Chinese Academy of Sciences, Hefei, Anhui, 230031, China. E-mail: cljiang@iim.ac.cn; zpzhang@iim.ac.cn
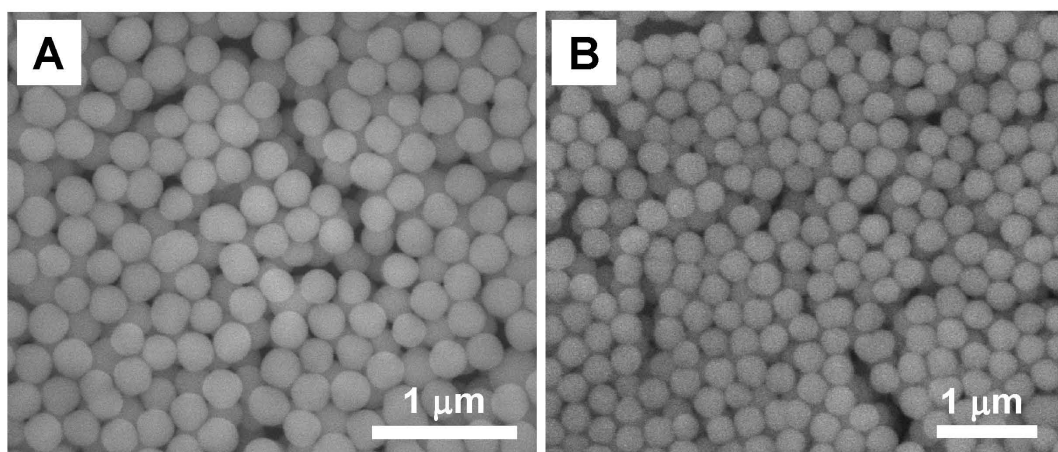
Figure S1. SEM images of the as-prepared SiO_2 nanospheres with the diameters of about 240 nm (a) and 300 nm (b) by adjusting the amount of the ammonia in the synthesis.
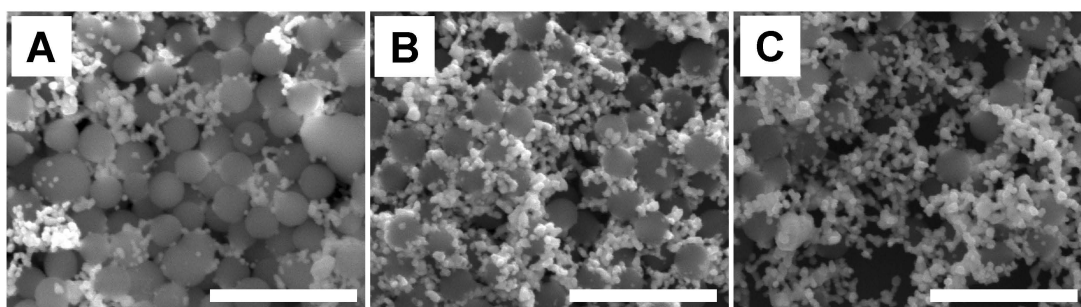

Figure S2. SEM images of Ag nanoparticles deposited on the silica nanospheres without modification prepared with different concentration of $AgNO_3$ (a) 1 mM, (b) 4 mM and (c) 8 mM. (scale bar is 500 nm)
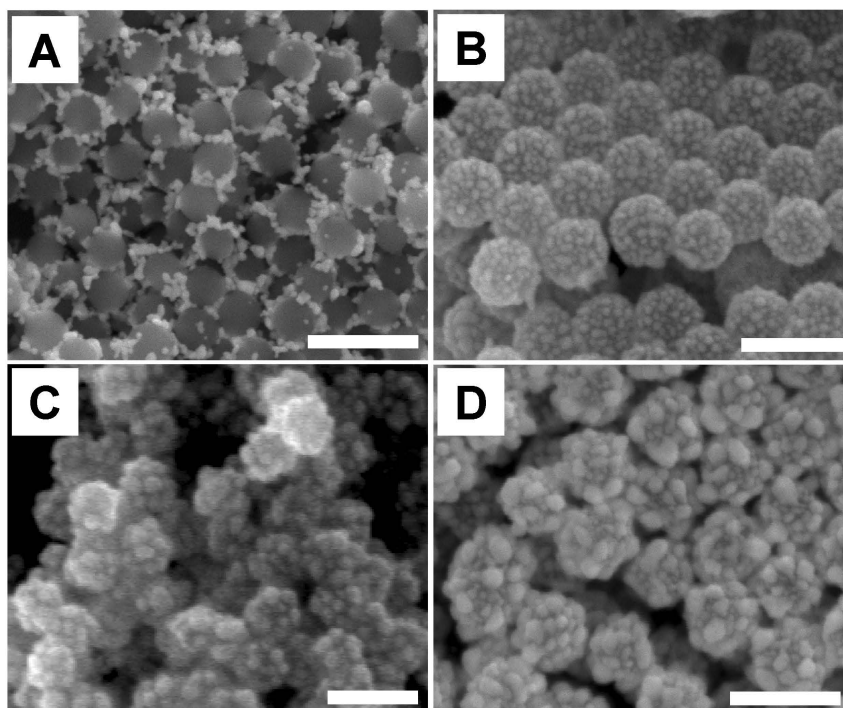
Figure S3. SEM images of Ag nanoparticles deposited on the silica nanospheres with modification with MPTMS prepared with different concentration of $AgNO_3$ (a) 1 mM, (b) 4 mM, (c) 6 mM and (d) 8 mM. (scale bar is 250 nm)
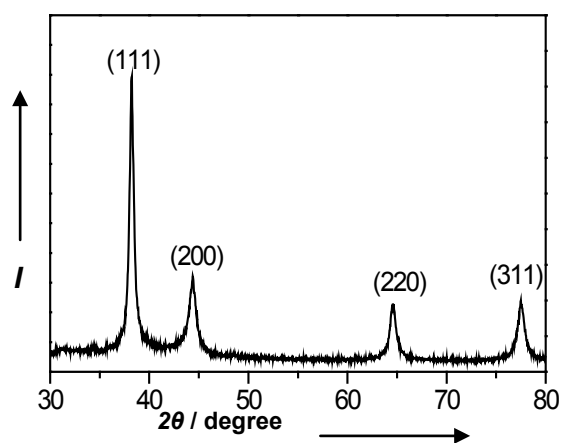

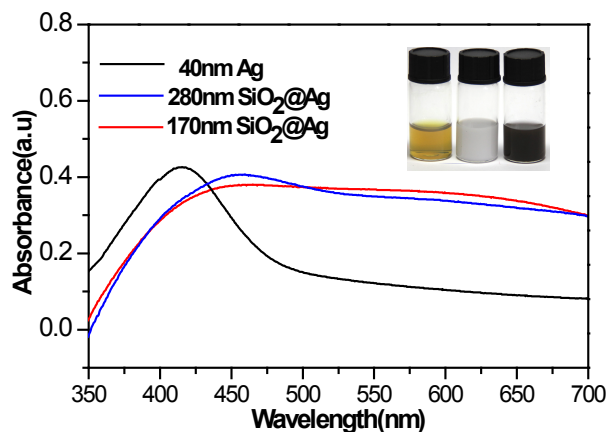Figure S4. XRD pattern of the as-synthesized 170 nm $SiO_2@Ag$ Nanospheres.

Figure S5. Uv-Vis spectra of 40 nm Ag nanoparticle colloids, 280 nm and 170 nm SiO_2@Ag nanospheres, respectively. Inserted are the digital photos of the 40 nm Ag nanoparticle colloids, bare SiO_2 nanospheres and SiO_2@Ag nanospheres (from left to right).
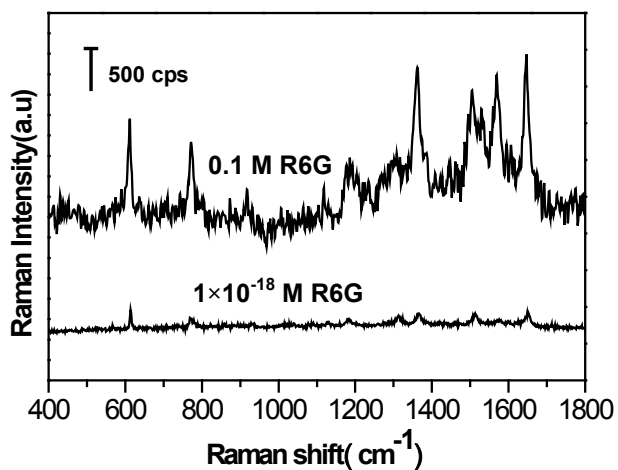

Figure S6. Raman spectra of 0.1 M R6G on a silicon substrate (upper) and 1×10^{-18} M R6G on the SiO_2@Ag NPs substrate (bottom), respectively.
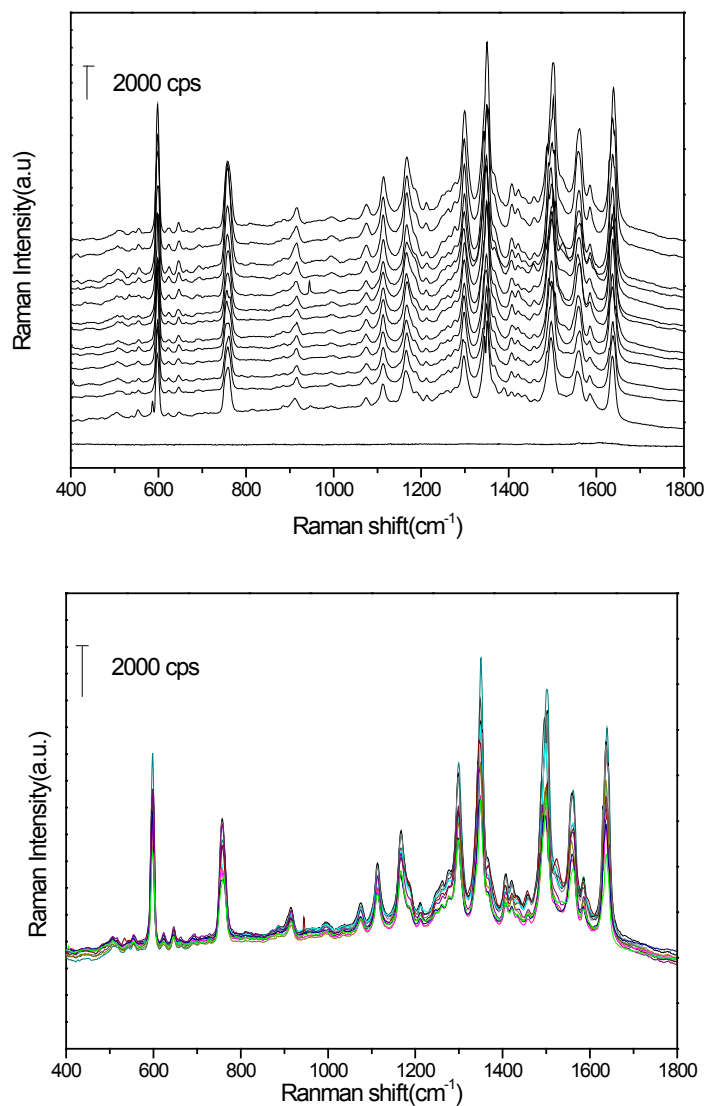
Figure S7. The SERS spectra of R6G from 13 random sites at the concentration of 1×10^{-12} M in ethanol by using the $SiO_2@Ag$ nanospheres as the enhanced substrate. The results indicated that the SERS platform exhibited good reproducibility and reliability for the detection.
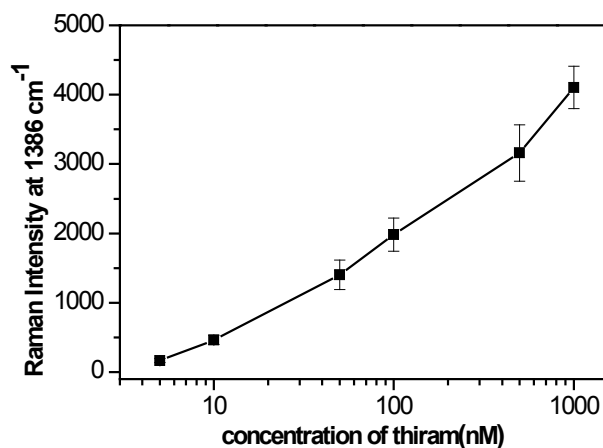
Figure S8. The intensities of SERS signals at 1386 cm^{-1} as the function of the concentrations of thiram in ethanol.
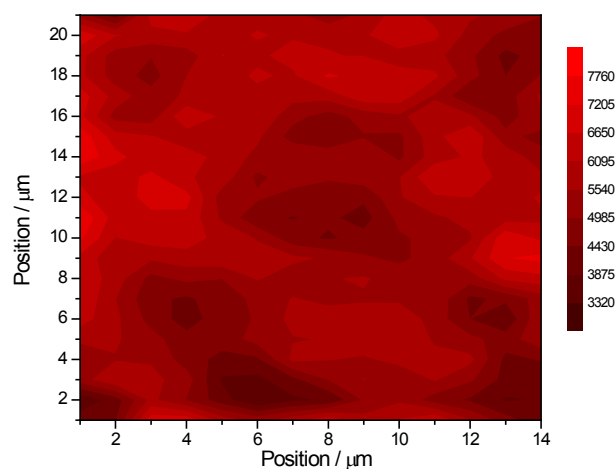

Figure S9. Raman mapping with the 1386 cm^{-1} band of the thiram at the concentration of 1×10^{-6} M in ethanol by using the $SiO_2@Ag$ nanospheres as the enhanced substrate. The result indicates that the SERS platform exhibited good reproducibility and reliability for the detection.
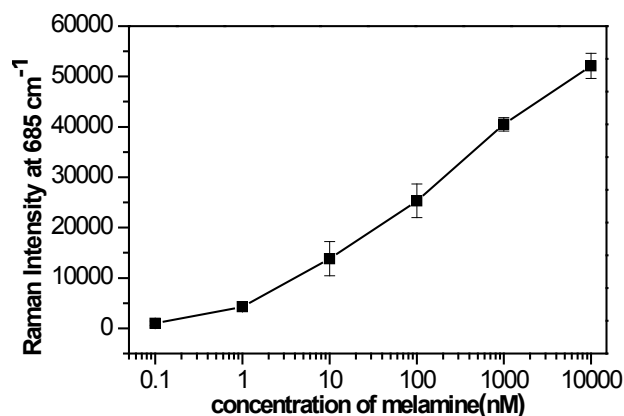
Figure S10. The intensities of SERS signals at 685 cm^{-1} as the function of the concentrations of melamine in ethanol.
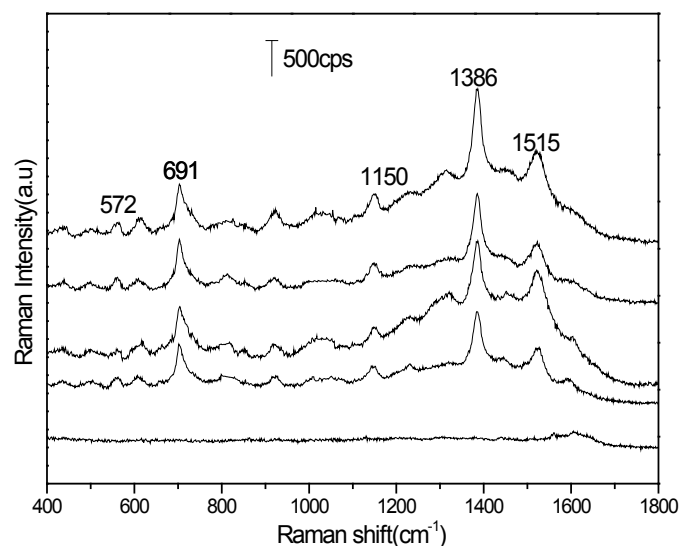

Figure S11. The SERS spectra of the multiple analytes at the concentration of 1×10^{-6} M in ethanol by using the $SiO_2@Ag$ nanospheres as the enhanced substrate (the bottom line represents the blank). The peaks at 1150, 1386 and 1515 cm^{-1} can be indexed to the "fingerprint" Raman spectra of thiram, and the peaks at 572 and 691 cm^{-1} suggested the presence of melamine in the samples. Therefore the SERS platform based on the $SiO_2@Ag$ nanospheres can be used to detect the multiple analytes at the same time.
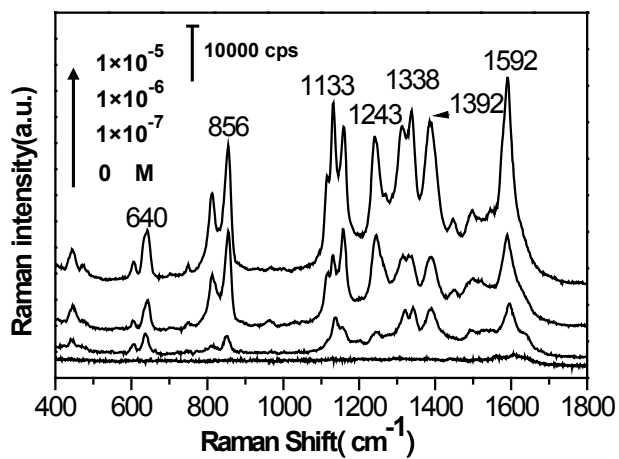
Figure S12. The SERS spectra of the ethyl-parathion in ultrapure water of various concentrations by using the SiO$_2$@Ag nanospheres as the enhanced substrate.
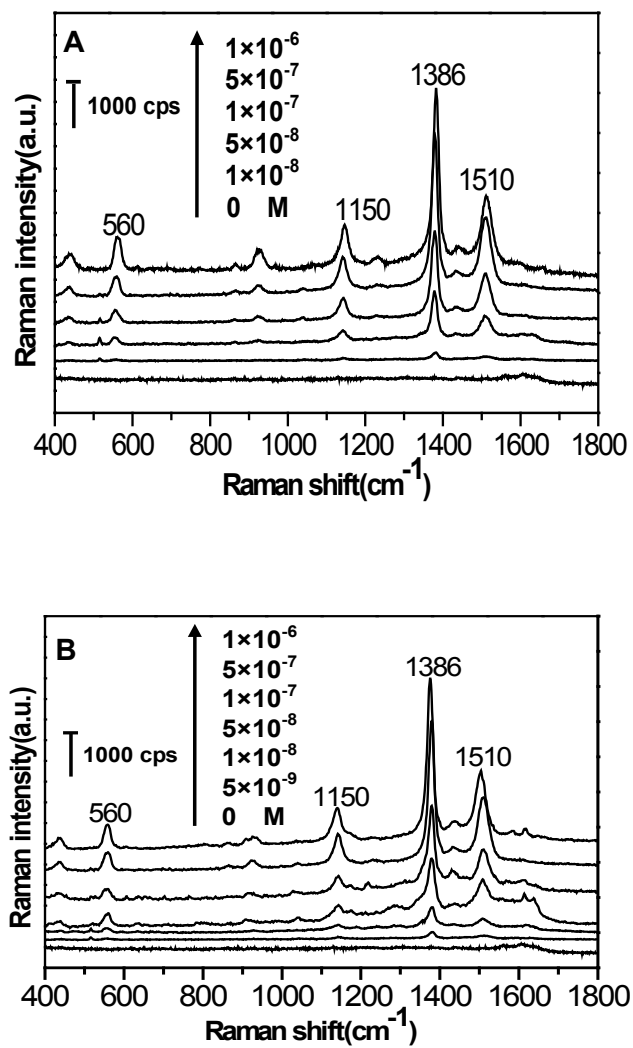
Figure S13. The SERS spectra of the thiram in ultrapure water (A) and lake water (B) of various concentrations by using the SiO_2@Ag nanospheres as the enhanced substrate.
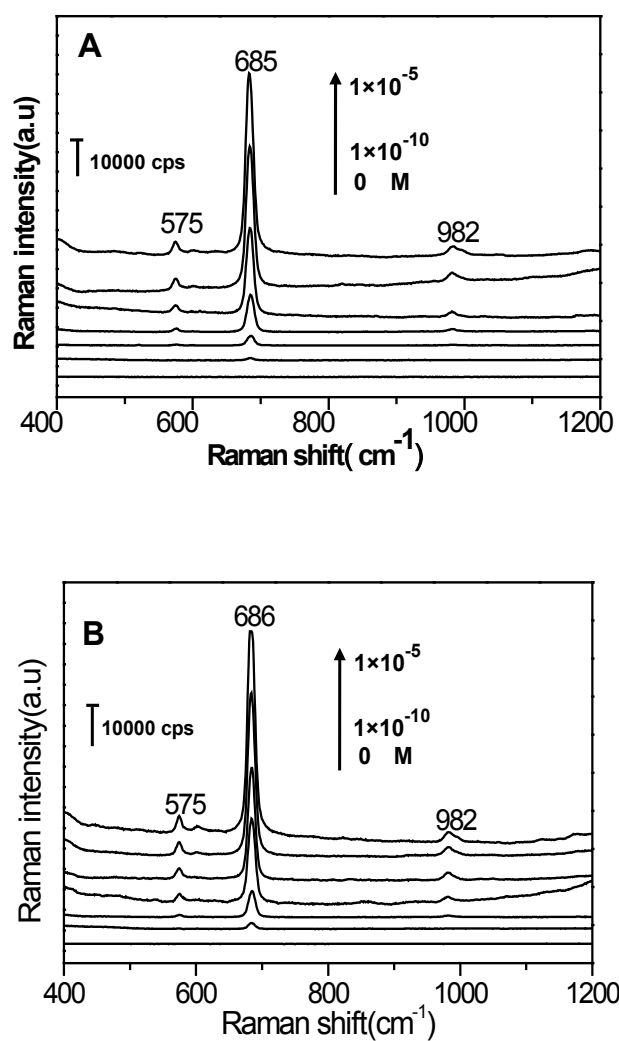
Figure S14. The SERS spectra of the melamine in ultrapure water (a) and lake water (b) of various concentrations by using the $SiO_2@Ag$ nanospheres as the enhanced substrate.
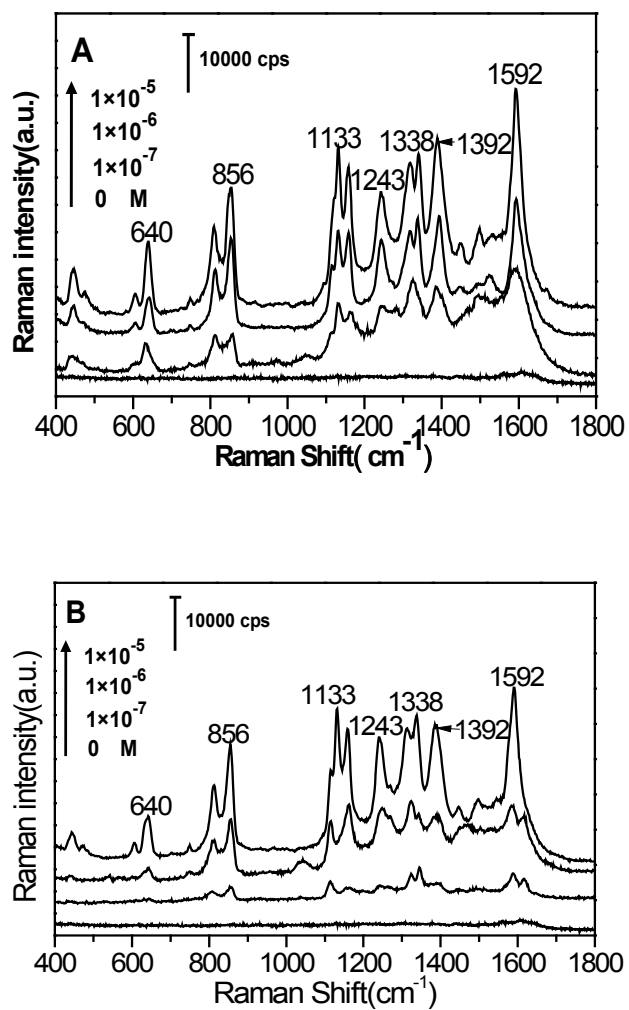
Figure S15. The SERS spectra of the ethyl-parathion in lake water (A) and pear juice (B) of various concentrations by using the SiO_2@Ag nanospheres as the enhanced substrate.